Combining symmetry breaking and restoration with configuration interaction: A highly accurate many-body scheme applied to the pairing Hamiltonian

J. Ripoche,[1,2,*] D. Lacroix,[1,†] D. Gambacurta,[3,‡] J.-P. Ebran,[2,§] and T. Duguet[4,5,6,‖]

[1]*Institut de Physique Nucléaire, IN2P3-CNRS, Université Paris-Sud, Université Paris-Saclay, F-91406 Orsay Cedex, France*
[2]*CEA, DAM, DIF, F-91297 Arpajon, France*
[3]*Extreme Light Infrastructure - Nuclear Physics (ELI-NP), Măgurele, Romania*
[4]*KU Leuven, Instituut voor Kern- en Stralingsfysica, 3001 Leuven, Belgium*
[5]*CEA, DRF/IRFU/SPhN, Université Paris-Saclay, 91191 Gif-sur-Yvette, France*
[6]*National Superconducting Cyclotron Laboratory and Department of Physics and Astronomy, Michigan State University, East Lansing, Michigan 48824, USA*

Background: Ab initio many-body methods have been developed over the past ten years to address mid-mass nuclei. In their best current level of implementation, their accuracy is of the order of a few percent error on the ground-state correlation energy. Recently implemented variants of these methods are operating a breakthrough in the description of medium-mass *open-shell* nuclei at a polynomial computational cost while putting state-of-the-art models of internucleon interactions to the test.

Purpose: As progress in the design of internucleon interactions is made, and as questions one wishes to answer are refined in connection with increasingly available experimental data, further efforts must be made to tailor many-body methods that can reach an even higher precision for an even larger number of observable quantum states or nuclei. The objective of the present work is to contribute to such a quest by designing and testing a new many-body scheme.

Methods: We formulate a truncated configuration-interaction method that consists of diagonalizing the Hamiltonian in a highly truncated subspace of the total N-body Hilbert space. The reduced Hilbert space is generated via the particle-number projected BCS state along with projected seniority-zero two- and four-quasiparticle excitations. Furthermore, the extent by which the underlying BCS state breaks U(1) symmetry is optimized *in the presence* of the projected two- and four-quasiparticle excitations. This constitutes an extension of the so-called restricted variation after projection method in use within the frame of multireference energy density functional calculations. The quality of the newly designed method is tested against exact solutions of the so-called attractive pairing Hamiltonian problem.

Results: By construction, the method reproduces exact results for $N = 2$ and $N = 4$. For $N = (8, 16, 20)$, the error in the ground-state *correlation energy* is less than (0.006%, 0.1%, 0.15%) across the entire range of internucleon coupling defining the pairing Hamiltonian and driving the normal-to-superfluid quantum phase transition. The presently proposed method offers the advantage of automatic access to the low-lying spectroscopy, which it does with high accuracy.

Conclusions: The numerical cost of the newly designed variational method is polynomial (N^6) in system size. This method achieves unprecedented accuracy for the ground-state correlation energy, effective pairing gap, and one-body entropy as well as for the excitation energy of low-lying states of the attractive pairing Hamiltonian. This constitutes a sufficiently strong motivation to envision its application to realistic nuclear Hamiltonians in view of providing a complementary, accurate, and versatile *ab initio* description of mid-mass open-shell nuclei in the future.

I. INTRODUCTION

Methods to solve the N-body Schrödinger equation must cope with two specific attributes of internucleon interactions that are responsible for the nonperturbative character of the nuclear many-body problem [1,2]. The first trait relates

───────

*julien.ripoche@cea.fr
†lacroix@ipno.in2p3.fr
‡danilo.gambacurta@eli-np.ro
§jean-paul.ebran@cea.fr
‖thomas.duguet@cea.fr

to the strong internucleon repulsion at short distances that translates into large off-diagonal coupling between states characterized by low and high (relative) momenta, i.e., the first element of nonperturbative physics is of ultraviolet nature and manifests itself in all nuclei independently of the detail of their structure. The second trait relates to the unnaturally large nucleon-nucleon scattering length in the S-wave and spin-singlet channel and with the tendency of internucleon interactions to induce strong angular correlations between nucleons in the internal frame of the nucleus. This second element of nonperturbative physics is of infrared character and only manifests itself in subcategories of nuclei, i.e., in singly open-shell and doubly open-shell nuclei.

Off-diagonal coupling between low and high (relative) momenta can be tamed down at the price of inducing (hopefully weak) higher-body forces by preprocessing the nuclear Hamiltonian via, e.g., a unitary similarity transformation [3]. Based on the transformed Hamiltonian, dynamical correlations[1] can be dealt with at a polynomial cost via standard many-body techniques typically based on systematic particle-hole-type expansions. Corresponding *ab initio* methods [i.e., many-body perturbation theory (MBPT) [4], coupled cluster (CC) theory [5], self-consistent Green's function (SCGF) theory [6,7], in-medium similarity renormalization group (IMSRG) theory [8]] have been developed and implemented with great success over the last ten years to deal with doubly (sub)closed shell nuclei and their immediate neighbors.

Strong, i.e., nondynamical, correlations induced in singly and doubly open-shell nuclei are of different nature and require specific attention. Several routes are possible, including full configuration-interaction (CI) techniques [9,10]. To proceed on the basis of methods whose cost scales polynomially with the number interacting nucleons, one option consists of exploiting the spontaneous breaking of symmetries induced by nondynamical correlations at the mean-field level. This rationale allows one to incorporate a large part of the non-perturbative physics into a single product state that can serve as a reference for many-body expansions dealing efficiently with dynamical correlations. While traditionally developed within the frame of effective nuclear mean-field (i.e., energy density functional) approaches [11–13], this idea has been recently embraced to develop and implement the *ab initio* Gorkov SCGF [14–16], multireference IMSGR [17,18], and Bogoliubov CC [19] many-body techniques to tackle pairing correlations.[2] This is achieved by allowing the reference state to break U(1) global gauge symmetry associated with particle-number conservation. While the restoration of the broken symmetry, eventually necessary in any finite quantum system, has been formulated for MBPT [24,25] and CC techniques [25], it has only been implemented so far in the context of nuclear *ab initio* calculations via MR-IMSGR techniques [17,18].

Methods based on a symmetry-breaking reference state are currently allowing a breakthrough in the *ab initio* description of (singly) open-shell nuclei and are putting state-of-the-art internucleon interactions to the test [16,26,27]. In the most advanced truncation schemes implemented so far, this is achieved by allowing a few percent error on the ground-state correlation energy.[3] As progress on internucleon interactions is made, and as the questions one wishes to answer are refined in connection with increasingly available experimental data, further efforts must be made to tailor many-body methods

(with minimized numerical costs) that can reach higher precision along with more observable quantum states or nuclei. The objective of the present work is to design and test a new many-body scheme that has the potential to do so.

To characterize the potential of new many-body schemes, one can test them against solutions of exactly solvable many-body Hamiltonians. To be in a position to draw meaningful conclusions, the schematic Hamiltonian must be significantly nontrivial and capture enough key physics of the real system of interest. In view of the above discussion, we presently focus on the so-called attractive pairing Hamiltonian [28–31] whose main merit is to effectively model the superfluid character of finite nuclear systems or any other mesoscopic fermionic superfluid system. More specifically, the dynamic of N interacting fermions is governed by the Hamiltonian

$$H(g) \equiv \sum_{k=1}^{\Omega} e_k (a_k^\dagger a_k + a_{\bar{k}}^\dagger a_{\bar{k}}) - g \sum_{k \neq l}^{\Omega} a_k^\dagger a_{\bar{k}}^\dagger a_{\bar{l}} a_l, \quad (1)$$

where Ω denotes the number of doubly degenerate ($e_k = e_{\bar{k}}$) time-reversed[4] single-particle states ($k, \bar{k}$) characterized by the creation operators ($a_k^\dagger, a_{\bar{k}}^\dagger$). The double degeneracy of single-particle states is meant to mimic (even-even) doubly open-shell nuclei treated via the spontaneous breaking of SO(3) rotational symmetry, i.e., exploiting explicitly the concept of deformation. In the present study, the distance between successive pairs of degenerate levels is constant, i.e., $e_{k+1} - e_k \equiv \Delta e$, and the system is systematically studied at "half filling," i.e., $N = \Omega$. Modeling, e.g., rare-earth nuclei, one typically has $\Delta e \sim$ 500 keV. The coupling strength $g \in [0, +\infty[$ characterizes the attractive pairing interaction that scatters pairs of nucleons from any given set of degenerate single-particle states to any other set with a constant probability amplitude. As g increases, the system is known to undergo a phase transition from a normal to a superfluid system at a critical value $g = g_c$ that depends on the number of particles N. Eventually, the relevant parameter of the model is the ratio $g/\Delta e$ that measures the pairing strength relative to the spacing between successive pairs of single-particle states. For rare-earth nuclei, one typically[5] has $g/\Delta e \sim 0.5$.

While the eigenstates of this Hamiltonian can be obtained exactly via direct diagonalization, i.e., full CI [32–34], quantum Monte Carlo simulations [35,36], or the numerical solution of the so-called Richardson equations [28–31,37,38], there exists a long history of search for accurate approximate solutions at the lowest possible algorithmic cost. Indeed, the numerical cost of exact methods scales factorial with N or Ω, which quickly becomes prohibitive for realistic systems of interest. Among these approximate methods[6] are the variation after particle-number projection Bardeen–Cooper–Schrieffer

---

[1]The denomination of *dynamical* and *nondynamical* correlations is presently used in the quantum chemistry sense.

[2]While the formation of Cooper pairs is primarily driven by the unnaturally large nucleon-nucleon scattering length in the spin-singlet isospin-triplet channel, it is also partly due to indirect processes associated with the exchange of collective vibrations [20–23].

[3]We are only quoting here the systematic uncertainty associated with the truncation of the many-body expansion scheme.

[4]The conjugation of the two single-particle states can actually originate from any dichotomic symmetry such as time reversal, signature, or simplex.

[5]Throughout the paper, numerical values quoted for g are in unit of Δe, i.e., they actually correspond to quoting the ratio $g/\Delta e$.

[6]We only focus here on methods that can be applied systematically for all coupling strength g, i.e., before, across, and after the

approach (VAP-BCS) approach [40–49], truncated CI calculations [50–52], and CC calculations without [39,53–56] or with U(1) symmetry breaking [19,57].

Particular attention must be paid to the highly accurate method recently proposed in Refs. [58,59]. Reconciling the performance of CC doubles in the normal phase with the merit of VAP-BCS in the strongly interacting regime, this method, coined "polynomial similarity transformation" (PoST), reaches less than 1% error:

$$(\Delta E/E)_c = \left(1 - \frac{E_c^{\text{approx}}}{E_c^{\text{exact}}}\right) \times 100\%, \qquad (2)$$

on the ground-state correlation energy E_c defined as the total energy minus the Hartree–Fock (HF) energy obtained by filling the N lowest levels, for all interaction strength and moderate particle number [59].

In view of this recent development, we presently wish to design a many-body scheme that scales polynomially with the number of interacting fermions and whose results display an error in the ground-state correlation energy that is better than 1% for any interaction strength. To reach this ambitious objective, the variational approach introduced below builds on Ref. [24] and combines two key characteristics:

    (1) U(1) symmetry breaking and restoration:
        (a) spontaneous,
        (b) optimized;
    (2) truncated CI diagonalization.

While Ref. [24] displays encouraging results by exploiting spontaneous U(1) symmetry breaking and restoration within a perturbative approach, the present work strongly improves on them by exploiting truncated CI techniques and by optimizing the extent by which the symmetry is broken prior to being restored. In addition, a strong asset of the presently proposed method is to provide a highly accurate account of low-lying excited states. The approach being based on a wave-function ansatz, observable besides the energy can easily be accessed as exemplified by the computation of the effective pairing gap and the one-body entropy.

This paper is organized as follows: Section II displays the formalism in such a way that several standard methods can be easily recovered as particular cases. Sections III–VI provide extensive numerical results and compare them with exact solutions as well as with those obtained from existing approximate methods. Eventually, results for low-lying excited states are discussed. Section VII concludes the present work and elaborates on some of its perspectives.

II. FORMALISM

A. Basis construction

We first consider the BCS solution for $H(g)$[7] carrying even number parity as a quantum number. It can be written as

$$|\Phi(g)\rangle \equiv \prod_{k=1}^{\Omega}(u_k(g) + v_k(g)a_k^\dagger a_{\bar{k}}^\dagger)|0\rangle, \qquad (3)$$

where the coefficients $(u_k(g), v_k(g))$ satisfying $u_k^2(g) + v_k^2(g) = 1$ for all k are obtained by solving standard BCS equations [60]. Quasiparticle creation operators, whose Hermitian conjugates annihilate $|\Phi(g)\rangle$, are obtained via the BCS transformation,

$$\beta_k^\dagger(g) \equiv u_k(g)a_k^\dagger - v_k(g)a_{\bar{k}}, \qquad (4a)$$

$$\beta_{\bar{k}}^\dagger(g) \equiv u_k(g)a_{\bar{k}}^\dagger + v_k(g)a_k. \qquad (4b)$$

Normal ordering $H(g)$ with respect to $|\Phi(g)\rangle$ allows one to rewrite it under the form

$$H(g) = H_0(g) + H_1(g), \qquad (5)$$

where the unperturbed part reads

$$H_0(g) = \mathcal{E}_0(g) + \sum_{k=1}^{\Omega} E_k(g)(\beta_k^\dagger \beta_k + \beta_{\bar{k}}^\dagger \beta_{\bar{k}}). \qquad (6)$$

The real number $\mathcal{E}_0(g)$ denotes the approximate BCS ground-state energy whereas

$$E_k(g) \equiv \sqrt{(e_k - \lambda)^2 + \Delta^2(g)} \qquad (7)$$

defines BCS quasiparticle energies, with $\Delta(g)$ being the BCS pairing gap [61]. The explicit expression of the residual interaction $H_1(g)$ can be obtained accordingly [60].

The BCS vacuum and the set of quasiparticle (qp) excitations built on top of it

$$|\Phi^{kl\cdots}(g)\rangle \equiv \beta_k^\dagger(g)\beta_l^\dagger(g)\cdots|\Phi(g)\rangle, \qquad (8)$$

form a complete eigenbasis $\mathcal{B}(g)$ of $H_0(g)$ over Fock space $\mathcal{F}$ such that

$$H_0(g)|\Phi(g)\rangle = \mathcal{E}_0(g)|\Phi(g)\rangle,$$
$$H_0(g)|\Phi^{kl\cdots}(g)\rangle = [\mathcal{E}_0(g) + E_k(g) + E_l(g) + \cdots]|\Phi^{kl\cdots}(g)\rangle.$$

Being interested in eigenstates of even-even systems with seniority zero, the only basis states of actual interest are those involving pairs of time-reversed quasiparticle excitations for which the shorthand notation

$$|\Phi^{k\bar{k}l\bar{l}\cdots}(g)\rangle \equiv |\Phi^{\breve{k}\breve{l}\cdots}(g)\rangle \qquad (9)$$

---

normal-to-superfluid phase transition. If not, more calculations could be mentioned, including those based on the self-consistent random-phase approximation [39] applicable to $g < g_c$.

---

[7]It is implicitly assumed here that the Hamiltonian is replaced by the grand potential $H(g) - \lambda A$, with λ being the chemical potential used to impose that the BCS solution has the right number of particles on average. The particle-number operator is $A = \sum_{k=1}^{\Omega}(a_k^\dagger a_k + a_{\bar{k}}^\dagger a_{\bar{k}})$.

is used. Eventually, all basis states can be written as BCS vacua of the form

$$|\Phi^{\check{k}\check{l}\cdots}(g)\rangle = \prod_{m=1}^{\Omega}\left(u_m^{\check{k}\check{l}\cdots}(g) + v_m^{\check{k}\check{l}\cdots}(g)a_m^\dagger a_{\bar{m}}^\dagger\right)|0\rangle. \quad (10)$$

This notation implicitly includes the BCS vacuum as a particular case when using the BCS coefficients $(u_m(g), v_m(g))$. For the excited state $|\Phi^{\check{k}\check{l}\cdots}(g)\rangle$, one has $u_m^{\check{k}\check{l}\cdots}(g) \equiv u_m(g)$ and $v_m^{\check{k}\check{l}\cdots}(g) \equiv v_m(g)$, except for $m = k, l, \ldots$ for which $u_m^{\check{k}\check{l}\cdots}(g) \equiv -v_m(g)$ and $v_m^{\check{k}\check{l}\cdots}(g) \equiv u_m(g)$.

While the eigenstates of $H_0(g)$ form a complete orthonormal basis of Fock space, they break the U(1) symmetry associated with particle-number conservation, i.e., they are not eigenstates of the particle-number operator A. To recover states belonging to the Hilbert space $\mathcal{H}_N$ associated with the physical number N of nucleons in the system, a projection operator

$$P_N = \frac{1}{2\pi}\int_0^{2\pi} d\varphi\, e^{i\varphi(A-N)} \quad (11)$$

can be applied to generate the set of projected qp excitations

$$|\Phi_N^{\check{k}\check{l}\cdots}(g)\rangle \equiv P_N|\Phi^{\check{k}\check{l}\cdots}(g)\rangle, \quad (12)$$

forming a nonorthogonal overcomplete basis $\mathcal{B}_N(g)$ of $\mathcal{H}_N$. While $|\Phi_N^{\check{k}\check{l}\cdots}(g)\rangle$ directly originates from $|\Phi^{\check{k}\check{l}\cdots}(g)\rangle$, the former is not an eigenstate of $H_0(g)$.

For $g > g_c$, each basis state defined through Eqs. (3)–(12) builds in the breaking of the U(1) symmetry prior to performing its exact restoration. As such, each state $|\Phi^{\check{k}\check{l}\cdots}(g)\rangle$ is a complex entanglement of 0p-0h, 2p-2h, ..., Np-Nh excitations with respect to the HF reference state, as nicely illustrated by Eq. (5) of Ref. [58]. For $g < g_c$, however, the BCS vacuum actually reduces to the HF reference state such that each state $|\Phi_N^{\check{k}\check{l}\cdots}(g)\rangle$ identifies with one n-particle–n-hole (np-nh) excitation on top of it belonging to $\mathcal{H}_N$.[8] Certain combinations of qp excitations do not actually have any np-nh counterpart in $\mathcal{H}_N$ for $g < g_c$. For example, a 2qp excitation of time-reversed states tend towards a Slater determinant belonging to $\mathcal{H}_{N\pm2}$ below g_c.

B. Truncated configuration-interaction method

We wish to approximate eigenstates of $H(g)$, starting with its ground state, via an exact diagonalization within the subspace of $\mathcal{H}_N$ spanned by a subset of states of $\mathcal{B}_N(g)$. A similar idea was used in a different context on the basis of projected quasiparticle random-phase approximation states [62] to estimate transfer probabilities between many-body states with different particle numbers. At this point, the present proposal displays great similarity to the broken pair approximation method [63] with two broken pairs and to the generalized seniority method with $v = 4$ [64]. However, a key difference will be introduced in Sec. II D below.

Eigenstates are approximated by the ansatz[9]

$$|\Psi_N(g)\rangle \equiv c|\Phi_N(g)\rangle + \sum_k c_{\check{k}}|\Phi_N^{\check{k}}(g)\rangle + \sum_{l<m} c_{\check{l}\check{m}}|\Phi_N^{\check{l}\check{m}}(g)\rangle, \quad (13)$$

i.e., it mixes the particle-number projected BCS vacuum with projected 2qp and 4qp excitations. The number of states in the linear combination is

$$\begin{aligned} n_{\text{st}} &= n_{\text{0qp}} + n_{\text{2qp}} + n_{\text{4qp}} \\ &= 1 + C_\Omega^1 + C_\Omega^2 \\ &= 1 + \Omega + \frac{\Omega(\Omega-1)}{2}, \end{aligned} \quad (14)$$

with $N = \Omega$ in the present application.

The many-body state is determined variationally

$$\delta\{\langle\Psi_N(g)|H(g)|\Psi_N(g)\rangle - E(g)\langle\Psi_N(g)|\Psi_N(g)\rangle\} = 0,$$

where the minimization is performed with respect to the set of coefficients $\{c_\alpha^*\} \equiv \{c^*, c_{\check{k}}^*, c_{\check{l}\check{m}}^*\}$, where α scans all states in the linear combination defining $|\Psi_N(g)\rangle$ in Eq. (13). This leads to n_{st} coupled equations[10]

$$\sum_\beta c_\beta \langle\Phi^\alpha(g)|H(g)|\Phi_N^\beta(g)\rangle = E(g)\sum_\beta c_\beta \langle\Phi^\alpha(g)|\Phi_N^\beta(g)\rangle. \quad (15)$$

Matrix elements of $H(g)$ between the basis states as well as the overlap between the latter can be estimated by using standard projection techniques. Explicit forms are given in the appendix of Ref. [24].

Equation (15) is nothing but the Schrödinger equation represented in a finite-size nonorthogonal basis. It is solved by first diagonalizing the overlap matrix through a unitary transformation $\mathcal{U}_N(g)$:

$$\sum_\beta \langle\Phi^\alpha(g)|\Phi_N^\beta(g)\rangle \mathcal{U}_N^{\beta\zeta}(g) = n_N^\zeta(g)\mathcal{U}_N^{\alpha\zeta}(g), \quad (16)$$

leading to a new set of orthonormal states

$$|\Theta_N^\zeta(g)\rangle \equiv \sum_\alpha \frac{\mathcal{U}_N^{\alpha\zeta}(g)}{\sqrt{n_N^\zeta(g)}}|\Phi_N^\alpha(g)\rangle, \quad (17)$$

which is eventually used to diagonalize $H(g)$. The number of new orthonormal states is of course equal to n_{st}. However, the size of the basis must actually be reduced prior to diagonalizing $H(g)$ by removing states with eigenvalues below a chosen threshold ϵ, i.e., states that encode the redundancy of the initial nonorthogonal overcomplete basis. We will illustrate this point in Sec. III C.

---

[8]In this case, the action of P_N is superfluous such that this is already true of the unprojected basis states $|\Phi^{\check{k}\check{l}\cdots}(g)\rangle$.

[9]The coefficient of the projected BCS vacuum is not set *a priori* because we keep the possibility to remove it altogether from the variational ansatz, in which case $c = 0$.

[10]Given that P_N is a projector ($P_N^2 = P_N$) and that $H(g)$ commutes with it ($[P_N, H(g)] = 0$), it is sufficient to apply the projector on only one of the two states involved in any matrix element of the overlap or Hamiltonian matrices. This is why we omit the subscript N in the bra $\langle\Phi^\alpha(g)|$ entering Eq. (15).

C. Particular cases

One must note that the above scheme incorporates several existing approaches as particular cases:

(1) When limiting ansatz (13) to the sole first term, one recovers the particle-number projection after the variation BCS (PAV-BCS) method. In this case, there is obviously no diagonalization to perform.

(2) For $g < g_c$, i.e., in the normal phase, the scheme reduces to a standard truncated CI method [50–52], limited to 2p-2h configurations in the present case.[11] In this case, the number of states does not comply with Eq. (18), i.e., it is replaced by

$$n_{\text{st}} = n_{0p0h} + n_{2p2h} = 1 + \left(C_{\Omega/2}^1\right)^2 = 1 + \frac{\Omega^2}{4}, \quad (18)$$

which for large Ω corresponds to essentially half of the cardinal defined in Eq. (18). The space spanned by the truncated basis is thus not continuous through g_c. Consequences will be discussed in Sec. III.

(3) When computing the mixing coefficients $\{c_\alpha\}$ from second-order (particle-number *unprojected*) MBPT, the diagonalization step is avoided. The residual interaction $H_1(g)$ contains terms with four quasiparticle operators[12] [60]. Consequently, $H_1(g)$ only couples the BCS vacuum $|\Phi(g)\rangle$ to 4qp excitations $|\Phi^{\bar{k}l}(g)\rangle$ at second order. As a result, coefficients $c_{\bar{k}}$ associated with 2qp excitations are identically zero at that order. Ansatz (13) can be both implemented in the *absence* of particle-number projection, in which case one works within a standard MBPT scheme, or in the *presence* of the particle-number projection, in which case one works within a particle-number projected MBPT scheme that we can coin as MBPT$_N$.[13] Of course, standard second-order MBPT based on a HF reference state is recovered from MBPT$_N$ at $g < g_c$. It happens that MBPT and MBPT$_N$ have been applied to the pairing Hamiltonian in Ref. [24] and serve as an inspiration for the generalizations introduced in the present work. Corresponding results will be briefly recalled in Sec. III.

D. Optimized order parameter

Let us introduce one additional level of improvement. At a given value of the coupling strength g, the states forming the nonorthogonal overcomplete basis $\mathcal{B}_N(g)$ have been naturally built so far from the BCS solution $|\Phi(g)\rangle$ of $H(g)$. Consequently, the extent by which $|\Phi(g)\rangle$ (possibly) break U(1) symmetry, as characterized by its pairing gap $\Delta(g)$, is in one-to-one correspondence with the coupling g defining the physical Hamiltonian. However, it is not at all obvious that the subpart of the resulting basis $\mathcal{B}_N(g)$ used in the truncated CI calculation optimally captures the physics of the Hamiltonian $H(g)$.

At each "physical" value g, it is thus possible to foresee the diagonalization of the Hamiltonian $H(g)$ in the (0qp, 2qp, 4qp) subpart of $\mathcal{B}_N(g_{\text{aux}})$ associated with an *auxiliary* value g_{aux}, i.e., with the basis built from the BCS solution $|\Phi(g_{\text{aux}})\rangle$ of an auxiliary pairing Hamiltonian $H(g_{\text{aux}})$.[14] Following this line of thinking, one can scan all values $g_{\text{aux}} \in [0,+\infty[$ in order to find the optimal auxiliary coupling g_{opt}. This extra step consists of spanning a larger manifold of states than when working at $g_{\text{aux}} = g$. The method is thus of variational character, i.e., the optimal auxiliary coupling g_{opt} is obtained at the minimum of the curve $E^{g_{\text{aux}}}(g)$ produced by repeatedly applying the truncated CI calculation, i.e., by solving Eq. (15) for the Hamiltonian $H(g)$ while varying the auxiliary coupling g_{aux} defining the basis states.

This scheme extends the so-called restricted variation after projection (RVAP) method designed within the frame of symmetry-restored nuclear energy density functional calculations [66]. A similar idea was also used in condensed matter [67] to study the t-J model and later in the Hubbard model [68]. Generally speaking, the idea is to scan the symmetry-restored energy as a function of a collective variable that monitors the extent by which the unprojected reference state breaks the symmetry. In the present case of U(1) symmetry, this order parameter is nothing but the pairing gap $\Delta(g_{\text{aux}})$ associated with the BCS reference state $|\Phi(g_{\text{aux}})\rangle$. Typically, tuning the value of the gap can be done by solving BCS equations while adding a Lagrange constrain term. In the present case, however, $\Delta(g_{\text{aux}})$ is a monotonic function of g_{aux} (see Fig. 9) such that one can directly use g_{aux} as a collective variable and solve for $H(g_{\text{aux}})$.

The novelty of the presently proposed scheme is that the optimal order parameter g_{opt} of the reference state is not only determined in the presence of the symmetry restoration but also in presence of the mixing with projected 2pq and 4qp states, i.e., at the level the truncated CI calculation itself. As discussed below, this significantly impacts the value of g_{opt} and the associated quality of the variational ansatz.

III. TRUNCATED CONFIGURATION-INTERACTION CALCULATIONS

A. Perturbation theory

For reference, we first illustrate MBPT and MBPT$_N$ methods employed in Ref. [24] and briefly introduced in

---

[11]As mentioned above, 2qp excitations of time-reversed states have no counterpart in $\mathcal{H}_N$ below g_c. Consequently, corresponding coefficients $c_{\bar{k}}$ are identically zero by construction in such a case.

[12]Terms with two creation or two annihilation operators are zero when $|\Phi(g)\rangle$ satisfies the BCS equations [19], i.e., in Møller–Plesset MBPT [65].

[13]The mixing coefficients $\{c_\alpha\}$ are still computed from MBPT without particle number projection. Note that an alternative particle-number-restored MBPT based on a projective formula has been recently proposed [25] but not yet applied.

---

[14]To some extent, performing standard truncated CI calculations based on a basis of np-nh Slater determinants already exploits this idea when dealing with $H(g)$ with $g > g_c$, i.e., it is nothing but using the basis $\mathcal{B}_N(g_{\text{aux}})$ built from the reference state corresponding to $g_{\text{aux}} < g_c$ in connection with a Hamiltonian $H(g)$ defined by $g > g_c$.
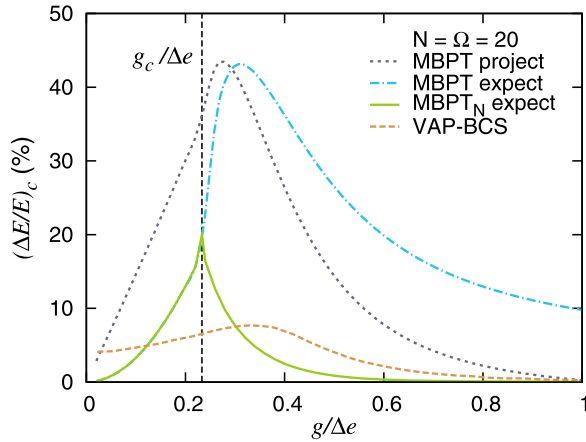
FIG. 1. Error $(\Delta E/E)_c$ in the ground-state correlation energy as a function of g for $N = \Omega = 20$. Results are shown for (i) second-order particle-number unprojected MBPT energy based on a projective formula (gray dotted line), (ii) second-order particle-number unprojected MBPT energy based on a Hermitian expectation value formula (blue dashed-dotted line), (iii) second-order particle-number projected MBPT$_N$ energy based on a Hermitian expectation value formula (green solid line), and (iv) for VAP-BCS [58] (brown dashed line). The critical value g_c is indicated by the black dashed vertical line.

Sec. II C above. Second-order results are displayed in Fig. 1 for $N = 20$ and compared with VAP-BCS results [58]. Three main lessons can be learned from these calculations:

(1) Second-order corrections avoid systematically the collapse of the correlation energy that occurs as g decreases through g_c in BCS or PAV-BCS calculations [48]. Of course, the VAP-BCS method also avoids the collapse but at the price of a significantly more sophisticated calculation.

(2) Particle-number projection drastically improves over unprojected results. Given that the standard Rayleigh–Schrödinger MBPT is based on a projective energy formula while MBPT$_N$ of Ref. [24] relies on a Hermitian expectation value, we also display the latter in the absence of the projection in order to disentangle its effect. For $g < g_c$, the improvement solely comes from using the expectation value formula given that the reference state does not break U(1) symmetry in the first place and thus the symmetry restoration cannot have any effect. For $g > g_c$, one sees that using the expectation-value formula does not improve the results by itself and even deteriorates the MBPT results obtained from a projective formula. Thus, the very significant improvement seen in the solid line does originate from the particle-number projection.

(3) Except in the vicinity of g_c, MBPT$_N$ results are better than VAP-BCS, both in the weak- and strong-coupling regimes. In particular, the results display the correct limit as $g \to 0$, contrary to VAP-BCS calculations [58]. This is not surprising given that standard second-order MBPT theory is known to converge to the right limit as g tends to zero. More surprisingly, MBPT$_N$ converges

very rapidly towards exact results as g increases beyond g_c. As a matter of fact, for $g > 0.6$, results are even better than the very accurate PoST approach of Ref. [59] that, by construction, matches VAP-BCS in the strong-pairing regime.

The quality of these results obtained at a low computational cost over both weakly and strongly coupled regimes teaches us that the space spanned by the states involved, i.e., the particle-number projected BCS vacuum and particle-number projected 4qp excitations, contain key information to treat the physics of superfluid systems. Indeed, the spontaneous breaking of the symmetry, followed by its further restoration, allows one to resum nondynamical correlations efficiently whereas corrections associated with 4qp excitations seem to capture a large part of the dynamical correlations. Still, results are significantly above the 1% error on the correlation energy that constitutes our present objective.

One natural generalization of the approach would be to include higher-order perturbative corrections. However, the rapid increase of the dimensionality of the probed Hilbert space translates into a severe augmentation of the computational cost. Alternatively, we move from a perturbative to a nonperturbative approach via a diagonalization method while keeping the dimensional of the probed Hilbert space essentially the same.

B. Diagonalization

At each g, $H(g)$ is diagonalized within the space spanned by the nonorthogonal set of projected 0qp, 2qp, and 4qp states built out of the BCS state $|\Phi(g)\rangle$, as explained in Sec. II B. The calculation reduces, as discussed in Sec. II C, to a diagonalization in a truncated basis made of 0p-0h and 2p-2h configurations built out of the HF reference state for $g < g_c$.

The error in the correlation energy is displayed in Fig. 2 for $N = \Omega = 16$. The diagonalization greatly improves the accuracy for $g > g_c$ compared with the perturbative calculation discussed above. The error is below the targeted 1% for all coupling beyond g_c and quickly drops far below it as g
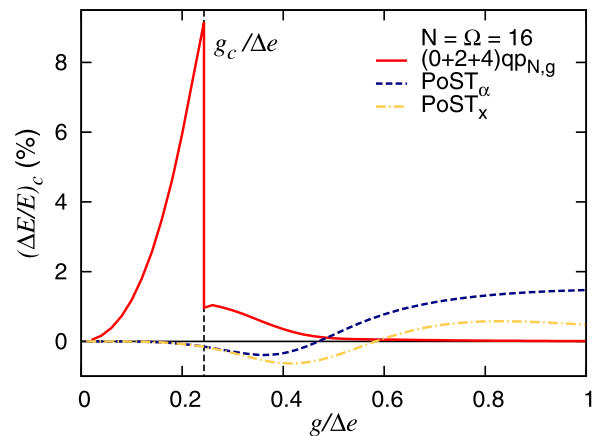

FIG. 2. $(\Delta E/E)_c$ as a function of g for $N = \Omega = 16$. Results are shown for the truncated CI (red solid line), PoST$_\alpha$ [59] (dark blue dashed line), and PoST$_x$ [59] (yellow dashed-dotted line) calculations.

moves away from the BCS threshold. Contrarily, results from the truncated CI calculation are similar to the perturbative calculation below the threshold. Eventually, a discontinuity of the result occurs at $g = g_c$.

The last feature can be qualitatively understood from the discontinuity of the basis dimension as g_c is approached from below or from above, as already alluded to in Sec. II C. By construction, the basis contains 0p-0h and 2p-2h Slater determinants of $\mathcal{H}_N$ below g_c. While a subset of 4qp states converges towards the 2p-2h Slater determinants when approaching g_c from above, others become more and more dominated by Slater determinants belonging to Hilbert spaces associated with neighboring (even) number of particles. Still, residual components corresponding to np-nh Slater determinants of $\mathcal{H}_N$ are extracted from them by projection. Consequently, the limit of the truncated CI calculation as g_c is approached from above corresponds to a standard truncated CI calculation associated with a basis containing higher-order np-nh Slater determinants beyond 2p-2h configurations, the basis size being approximately twice that below threshold. This feature greatly improves the quality of the method and illustrates the benefit of starting from symmetry-broken (and restored) basis states above g_c.

Eventually the proposed method is competitive with the PoST method of Ref. [59] and becomes even quickly superior as one enters the strongly coupled regime. Still, the strict reduction of the method to a truncated CI based on sole 0p-0h and 2p-2h configurations below g_c is not sufficient to reach the desired accuracy across both normal and superfluid phases and to obtain a smooth description throughout the transition. In Sec. IV below, this intrinsic limitation is overcome while further improving the accuracy for all g. Before discussing this additional level of improvement, let us first focus on the redundant character of the basis and of the optimal set of qp configurations one should start from.

C. Basis redundancy and quasiparticle configurations

Based on unprojected MBPT, it is natural to first add 4qp excitations to the BCS reference state in the variational ansatz $|\Psi_N(g)\rangle$. The argument that the BCS reference state is not coupled to 2qp excitations via the residual interaction $H_1(g)$ does not, however, stand once the particle-number projector is inserted; thus, our additional inclusion of 2qp excitations in the variational state $|\Psi_N(g)\rangle$. The final set of projected 0qp, 2qp, and 4qp states is not orthonormal and thus contains a certain degree of redundancy. As explained in Sec. II B, this requires the diagonalization of the overlap matrix to extract a subset $n_{\text{sub}} \leqslant n_{\text{st}}$ of relevant orthonormal states characterized by sufficiently large eigenvalues $n_N^\zeta(g) \geqslant \epsilon$. Let us now typify the relevant states depending on the original set of configurations included in the variational ansatz and characterize at the same time the quality of the associated results. We still focus on the $N = 16$ case.

The upper panel of Fig. 3 displays the $n_{\text{st}} = 1 + 16 + 120 = 137$ eigenvalues $n_N^\zeta(g)$ of the overlap matrix from the full set of projected 0qp, 2qp, and 4qp configurations. Employing a logarithmic scale and ordering the eigenvalues increasingly, one observes that they gather in two distinct
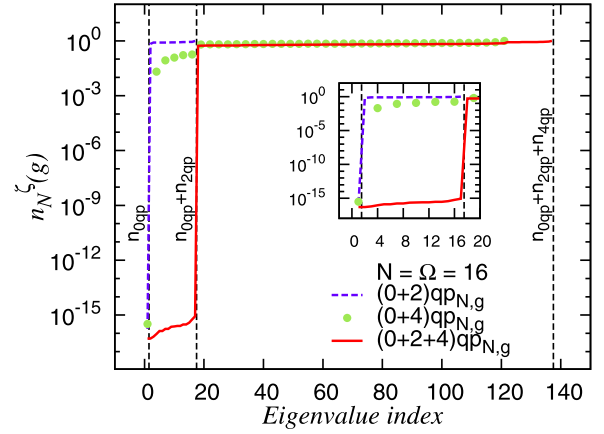

FIG. 3. Eigenvalues $n_N^\zeta(g)$ (relative to the largest of them) of the overlap matrix [cf. Eq. (16)] ordered in increasing values for $N = 16$ and $g/\Delta e = 0.8$. A logarithmic scale is used for the vertical axis. Results are shown for $|\Psi_N(g)\rangle$ made of projected 0qp, 2qp, and 4qp configurations (red solid line), made of projected 0qp and 4qp configurations (green filled circles) or made of projected 0qp and 2qp configurations (purple dashed line).

groups, i.e., one finds $17 = n_{0\text{qp}} + n_{2\text{qp}}$ very small eigenvalues consistent with numerical noise and $120 = n_{4\text{qp}}$ values of order unity. Very naturally, the threshold is set such that only the latter eigenstates are kept to eventually diagonalize the Hamiltonian. Naively, the observation that the number of useful orthonormal states is strictly equal to the cardinal of projected 4qp states may suggest that the latter capture from the outset the information contained in the set of 0qp and 2qp configurations. Let us now investigate this hypothesis.

Removing all 2qp configurations from the calculations, the middle panel of Fig. 3 shows that only one small eigenvalue remains while $120 = n_{4\text{qp}}$ of them are still of order unity. Additionally, the upper panel of Fig. 4 testifies that the error on the correlation energy is the same as in the presence of projected 2qp configurations, which indeed appear to be redundant and can be entirely omitted from the outset. For large bases and/or particle number, the numerical scaling is governed by the number of 4qp configurations such that omitting projected 2qp excitations does not lead to a significant gain. Having one zero eigenvalue left, one may be tempted to conclude that the projected BCS reference state can be further removed from the linear combination. However, and as shown in the lower panel of Fig. 4, the error in the correlation energy is huge for $g > g_c$ in this case. Thus, projected 4qp configurations do not fully contain the information built into the projected BCS state such that the useful set of $n_{\text{st}} - 1 = n_{4\text{qp}}$ orthonormal states do mix in a significant fraction of the projected 0qp state that cannot be plainly omitted. Ironically, bringing back projected 2qp configurations while keeping the projected BCS state aside is sufficient to gain back the accuracy of the calculation based on projected 0qp and 4qp configurations, i.e., the set of projected 2qp configurations do bring in the mandatory information otherwise contained in the projected 0qp state. Of course, it is more efficient to do it by including one 0qp state rather than sixteen 2qp configurations.
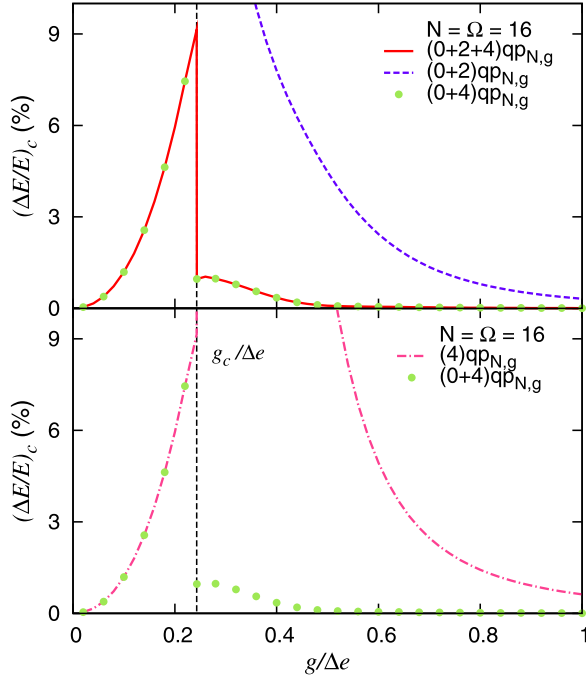
FIG. 4. $(\Delta E/E)_c$ from truncated CI calculations as a function of g for $N = \Omega = 16$. Upper panel shows results for the full set of projected 0qp, 2qp, and 4qp configurations (red solid line) as well as using 0qp and 4qp (green filled circles) or 0qp and 2qp (purple dashed line) configurations only. Lower panel shows results for 0qp and 4qp configurations (green filled circles) as well as for 4qp configurations only (pink dashed-dotted line).

To eventually confirm that all combinations of projected states are not equivalent, let us finally keep projected 0qp and 2qp configurations while omitting projected 4qp configurations. In this case, one is left with $16 = n_{2qp}$ eigenvalues of order unity and a null one as shown in Fig. 3. As for the error in the correlation energy, the results are, however, much inferior to the full calculation, as seen in the upper panel of Fig. 4.

In conclusion, the information carried by projected 4qp states cannot be brought in by lower-order projected qp configurations while the opposite is true to some extent.

IV. OPTIMIZED ORDER PARAMETER

As described in Sec. II D, the order parameter of the BCS reference state associated with the underlying breaking of U(1) symmetry can be optimized, for each "physical" g of interest, when applying the truncated CI method. To do so, the diagonalization of $H(g)$ is repeated while scanning g_{aux} [i.e., $\Delta(g_{aux})$] that parametrizes the truncated basis until the minimum of the lowest eigenenergy $E^{g_{opt}}(g)$ is found.

A. Projection after variation BCS ansatz

As a jump-start, the rationale is first applied while restricting the trial state to the first term in Eq. (13), i.e., to the PAV-BCS wave function. This strictly corresponds to the RVAP method designed within the frame of multireference
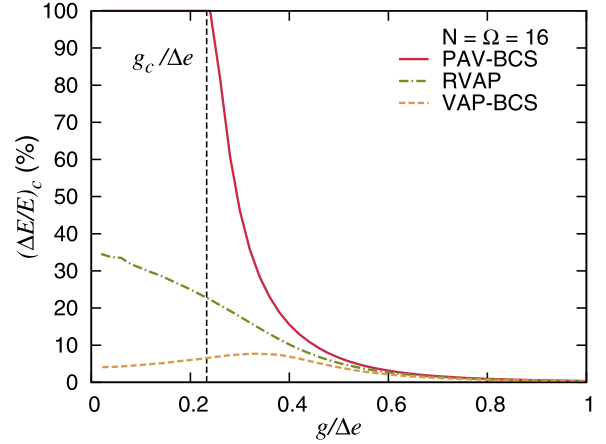

FIG. 5. $(\Delta E/E)_c$ as a function of g for $N = \Omega = 16$. Results are shown for the the VAP-BCS (brown dashed line), the standard PAV-BCS (dark red solid line), and for a PAV-BCS calculation based on an optimized order parameter (dark green dashed-dotted line). The latter corresponds to the RVAP method.

nuclear energy density functional calculations [66]. Results as a function of g are compared in Fig. 5 to actual PAV-BCS and VAP-BCS results. By definition, PAV-BCS results are generated by setting $g_{aux} = g$ for each given g, i.e., by picking the order parameter obtained at the level of the BCS wave function rather than at the level of the actual PAV-BCS wave function.

While the results are not at the desired level because of the lack of projected qp excitations, they perfectly illustrate the gain induced by optimizing the order parameter at the level of the full calculation, i.e., after the symmetry restoration is performed in the present example rather than prior to it. It is particularly striking below threshold where $(\Delta E/E)_c$ decreases from 100% to about 20%–40%. In the normal phase, not too far from the BCS threshold, it is indeed highly beneficial to allow the reference state to break U(1) symmetry while restoring it. As discussed above, this corresponds to including a specific set of np-nh configurations at a low computational cost. This reduced set provides an efficient way to partly capture correlations associated with pairing fluctuations that arise as a precursor of the phase transition. Above threshold, results are also significantly improved over the range $g \in [g_c, 0.4]$ by finding the optimal order parameter. For $g > 0.6$, no significant gain is obtained given that PAV-BCS itself becomes eventually exact.

One interest of this optimization is that the associated numerical effort simply corresponds to repeating the full calculation a few number of times. At the PAV level, it makes the RVAP calculation inexpensive compared with the VAP-BCS calculation that it approximates. Of course, results are significantly less accurate than the actual VAP-BCS calculation given that the optimization of the order parameter is not equivalent to exploring the complete manifold of BCS states as in the VAP-BCS calculation. This is particularly true in the very-weak-coupling regime where the system does not experience pairing fluctuations.
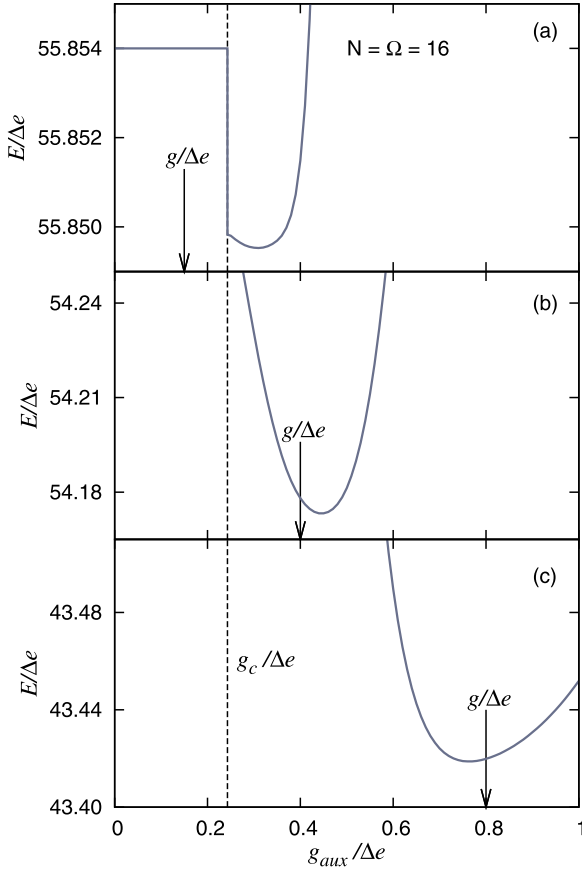
FIG. 6. Total binding energy from truncated CI calculations based on projected 0qp, 2qp, and 4qp configurations as a function of g_{aux}. The calculations are performed for $N = \Omega = 16$ and the specific value of g indicated by the arrow. (a) $g = 0.15 < g_c$. (b) $g = 0.4 > g_c$. (c) $g = 0.8 \gg g_c$.

B. Full ansatz

The rationale is now implemented on the basis of the full ansatz of Eq. (13). Figure 6 displays the so-called potential-energy surface (PES) representing the total energy $E^{g_{aux}}(g)$ as a function of g_{aux}. Results are given for three representative values of g, i.e., $g = 0.15 < g_c$ [Fig. 6(a)], $g = 0.4 > g_c$ [Fig. 6(b)], and $g = 0.8 \gg g_c$ [Fig. 6(c)].

In each case, the minimum of the PES indicates the position of g_{opt}. One first notices that the minimum of the curve is typically not obtained for $g_{aux} = g$. The optimal basis in presence of the configuration mixing is characterized by a symmetry breaking, i.e., a reference pairing gap $\Delta(g_{opt})$ that differs from the one obtained at the (projected) BCS minimum. This is particularly striking for $g < g_c$ (upper panel of Fig. 6) where it is advantageous to employ a basis that explicitly captures features of pairing fluctuations, i.e., that benefits from the additional np-nh configurations brought about by projected 0qp, 2qp, and 4qp states. Beyond the phase transition, one has $g_{opt} > g$ ($g_{opt} < g$) for intermediate (large) coupling as exemplified in the middle (lower) panel of Fig. 6. All in all, the successive inclusion of the particle-number restoration and of the qp excitations significantly influence the value of g_{opt} and the associated quality of the variational ansatz (see

TABLE I. Optimal order parameter g_{opt} of the reference state at various levels of approximation, i.e., BCS, PAV-BCS, and truncated CI calculation based on projected 0qp, 2qp, and 4qp configurations, for $N = 16$. Results are provided for $g = 0.15 < g_c$, $g = 0.40 > g_c$, and $g = 0.80 \gg g_c$. Recall that $g_c = 0.24$ for $N = 16$.

g	BCS	PAV-BCS	Truncated CI
0.15	0.15	0.29	0.31
0.40	0.40	0.44	0.45
0.80	0.80	0.82	0.76

below), especially at weak and intermediate coupling. This is summarized in Table I.

Figure 7 provides the same comparison as Fig. 2 but with the optimal order parameter g_{opt} defining the basis at each value of the coupling g. The optimization generates an impressive systematic improvement for $g < 0.6$ and solves completely the discontinuity problem observed in Fig. 7 at $g = g_c$. The error on the correlation energy is now lower than 0.1% for all g, which is almost one order of magnitude lower than our original goal. Our results compare very favorably with PoST methods [58,59]. Once again, projected 2qp configurations are redundant and can actually be omitted.

Figures 8(a) and 8(b) display similar results for $N = \Omega = 8$ and (b) $N = \Omega = 20$, respectively. The conclusions are essentially the same as for $N = \Omega = 16$.

V. PERFORMANCE AND SCALING

The main feature of the presently proposed method resides in the optimization of the basis used to diagonalize the Hamiltonian. This results in a dimensionality that is drastically reduced compared with the total Hilbert space and, for a given accuracy, compared with truncated CI calculations based on traditional np-nh configurations. The rationale of the latter method is to describe the system via a basis of product states that respect U(1) symmetry even in the superfluid phase. The
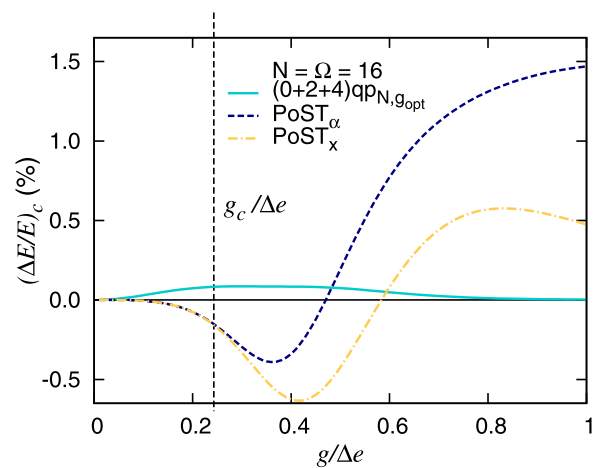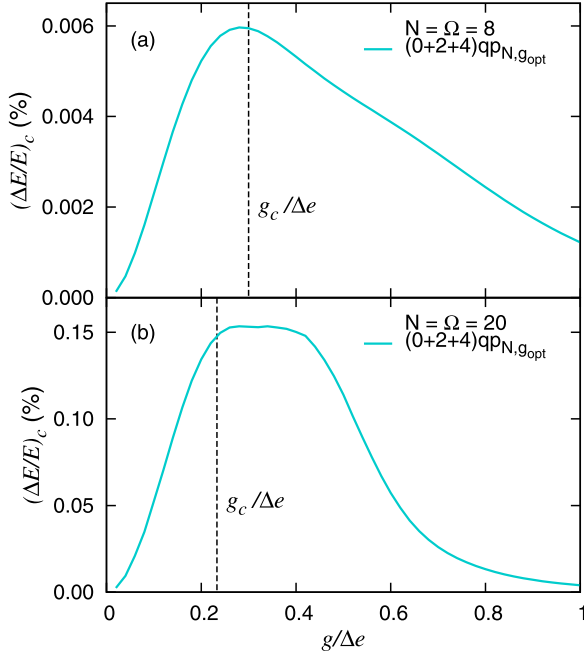

FIG. 7. Same as Fig. 2 but with the optimal order parameter g_{opt} defining the basis at each value of the coupling g for the truncated CI (light blue solid line). Results of PoST$_\alpha$ (dark blue dashed line) and PoSTx [59] (yellow dashed-dotted line) are shown for comparison.

FIG. 8. Same as Fig. 7 for (a) $N = \Omega = 8$ and (b) $N = \Omega = 20$.

rationale of our method is exactly opposite, i.e., it uses a basis that exploits the breaking of U(1) symmetry (while restoring it) to describe the system even in its normal phase.

Table II compares, for $N = 16$, the total size of $\mathcal{H}_N$ with the cardinal of the basis employed in standard np-nh truncated CI calculations up to 8p-8h [52], as well as in the presently designed approach. The corresponding error on the correlation energy is provided for $g = 0.18$, $g = 0.54$, and $g = 0.66$. We recall in passing that the dimension of the basis used in truncated CI calculations based on the 0qp and 4qp configurations makes the method exact for $N = 2$ and $N = 4$.

In the weak-coupling regime ($g = 0.18$), truncated CI calculations based on the 0p-0h and 2p-2h configurations

TABLE II. Dimensionality n_{st} of the full N-body Hilbert space $\mathcal{H}_N$ for $N = \Omega = 16$ as well as of the subspace considered in np-nh truncated CI calculations as well as in our method. In each case, the last three columns display the error on the correlation energy for $g = 0.18$, $g = 0.54$, and $g = 0.66$, respectively.

$N = 16$	n_{st}	$g = 0.18$	$g = 0.54$	$g = 0.66$
2p-2h	65	0.64%	20.92%	29.37%
4p-4h	849	0.01%	5.22%	9.59%
6p-6h	3985	0.00%	0.60%	1.66%
8p-8h	8885	0.00%	0.03%	0.12%
$(0+2)\text{qp}_{N,g}$	17	100%	3.52%	1.70%
$(0+4)\text{qp}_{N,g}$	121	0.64%	0.07%	0.04%
$(0+2+4)\text{qp}_{N,g}$	137	0.64%	0.07%	0.04%
$(0+2)\text{qp}_{N,g_{\text{opt}}}$	17	9.20%	3.34%	1.66%
$(0+4)\text{qp}_{N,g_{\text{opt}}}$	121	0.07%	0.07%	0.03%
$(0+2+4)\text{qp}_{N,g_{\text{opt}}}$	137	0.07%	0.07%	0.03%
Exact	12870	0.00%	0.00%	0.00%

already achieve an error below 1% based on a small basis size, which eventually scales as N^2 with system size. Calculations based on optimized projected 0qp and 4qp configurations perform one order of magnitude better based on a basis that is only twice as large and that scales similarly with system size. If degrading the calculation to optimized projected 0qp and 2qp configurations, a scheme that scales as N with the system size, the result are, however, one order of magnitude worse (10% error on E_c) than the CI calculation based on the 0p-0h and 2p-2h configurations. This demonstrates the need to include 4qp configurations to reach (much) better than the 1% accuracy at weak coupling.

In the superfluid regime, truncated CI calculations based on projected 0qp and 4qp configurations reach again an accuracy well below 1%, which is comparable to the results obtained from truncated CI calculations including up to 8p-8h configurations for $g = 0.54$ and is even one order of magnitude better for $g = 0.66$. While the dimension of the latter basis scales as N^8 with the system size, the set of projected 0qp and 4qp configurations scales as N^2, which is obviously much more gentle. For rather strongly paired systems, i.e., for $g = 0.66$, degrading the calculation to optimized 0qp and 2qp configurations, which scales as N with the system size, already reaches 1% accuracy in the correlation energy.

Of course, part of the cost of the calculation is transferred into the particle-number projection but the end scaling is still very favorable. Eventually, the numerical cost $\text{Num}(N)$ of the scheme is polynomial and scales according to

$$\text{Num}(N) = n_{g_{\text{aux}}}(\text{BCS}(g_{\text{aux}}, N) + n_{\text{st}}^2 \, \text{ME}(n_\phi, N) + \text{DIAG}(n_{\text{st}})), \quad (19)$$

where the first term relates to solving BCS equations, the second term to calculating the elements of the overlap and Hamilton matrices, and the third term designates the cost of the diagonalization of these two matrices.

The cost scales linearly with the number of times $n_{g_{\text{aux}}}$ the calculation must be performed to find the optimal g_{opt}. In practical calculations, it is possible to keep $n_{g_{\text{aux}}} < 10$ once the calculation at $g_{\text{aux}} = g$ has been performed. Of course, $n_{g_{\text{aux}}} = 1$ when the optimization of the order parameter characterizing the basis is omitted.

The cost associated with the BCS variation is negligible because it scales essentially linearly with $\Omega = N$. Employing projected 0qp and 4qp (2qp) configurations, the number of matrix elements n_{st}^2 to calculate scales as N^4 (N^2) while the cost of their computation is $\text{ME}(n_\phi, N) = \alpha n_\phi N^2$, which makes the overall scaling go as $n_\phi N^6$ ($n_\phi N^4$). The cost of computing the matrix elements is linear with the number of gauge angles n_ϕ employed in the particle-number projector [see Eq. (11)]. This number can be kept essentially constant, i.e., $n_\phi \sim 10$, when increasing N. Finally, the cost of the diagonalization is $\text{DIAG}(n_{\text{st}}) = \beta n_{\text{st}}^3 = \beta N^6$ (βN^3).

All in all, the building of the matrices and their diagonalization scale similarly as N^6 (the building of the matrix goes as N^4 and dominates when using projected 0qp and 2qp configurations) with system size. There are ways to further improve on this situation. First, full diagonalization is not mandatory because one can envision the use of alternative

methods such as Lanczos to extract a few low-lying states at a much-reduced numerical cost. This might be particularly useful when addressing large model spaces and/or particle numbers associated with realistic cases of interest. Second, the prefactor αn_ϕ associated with the direct integration over the gauge angle to perform the particle number projection can be scaled down by performing the latter on the basis of recurrence relations [69].

Last but not least, there probably is a systematic convergence of the result, as in standard truncated CI calculations [52], as a function of the maximum unperturbed energy of the 2qp and 4qp included in the ansatz for a given single-particle basis size (Ω here). This means that, given a targeted accuracy, the dimensionality and the numerical cost might be significantly scaled down by exploiting this additional convergence parameter and complementing the calculation by an appropriately designed formula to extrapolate the results to the untruncated limit. Such a systematic study has not been performed within the scope of the present paper but could be envisioned in the future.

VI. ADDITIONAL OBSERVABLES

To complete our study, the discussion is extended to other observables.

A. Effective pairing gap

We start with the computation of the effective pairing gap [70,71]

$$\Delta_{\text{eff}}(g) = g \sum_{k=1}^{\Omega} \sqrt{\langle a_k^\dagger a_{\bar{k}}^\dagger a_{\bar{k}} a_k \rangle - \frac{1}{4} \langle (a_k^\dagger a_k + a_{\bar{k}}^\dagger a_{\bar{k}}) \rangle^2}, \quad (20)$$

which generalizes the BCS gap $\Delta(g)$ and where the expectation values are to be computed for any ground-state wave function of interest.

In Fig. 9, the effective gap obtained in the exact case is compared with that obtained from various approximate many-body methods of present interest. We observe that truncated CI calculations based on (non)optimized projected 0qp and 4qp configurations provide results that are below 0.05% (1.5%) error for all coupling strengths g ($g > g_c$) and are much superior to the other methods shown.

B. One-body entropy

States obtained via the presently proposed method are strongly entangled in the sense that they correspond to a complex mixing of independent-particle states. As a matter of fact, exact solutions are known to be highly correlated states, resulting into extended diffusion of single-particle occupation numbers across the Fermi energy. To quantify the deviation of these many-body states from any independent-particle state, the single-particle entropy defined as

$$\frac{S}{k_B} = -2 \sum_{k=1}^{\Omega} \{\langle a_k^\dagger a_k \rangle \ln \langle a_k^\dagger a_k \rangle + (1 - \langle a_k^\dagger a_k \rangle) \ln(1 - \langle a_k^\dagger a_k \rangle)\}$$
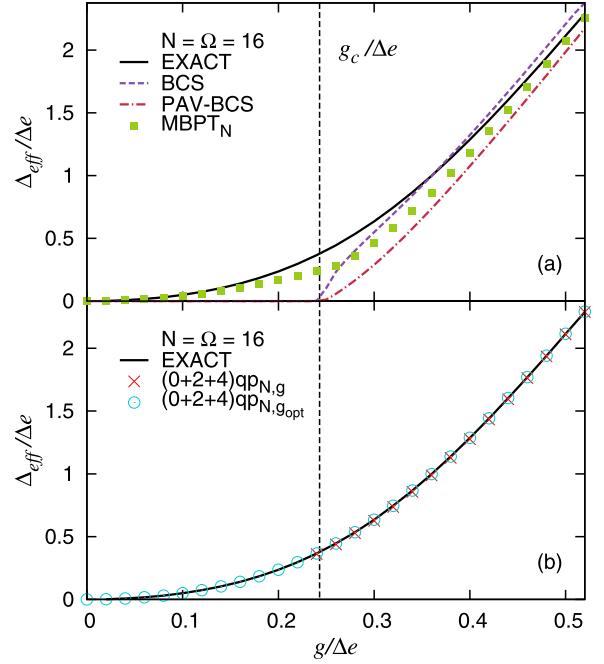
$$(21)$$

FIG. 9. Ground-state effective pairing gap [Eq. (20)] as a function of g for $N = 16$. Top panel shows exact results (black solid line) against BCS (purple dashed line), PAV-BCS (red dot-dashed line), and MBPT$_N$ (green filled squares). Lower panel shows exact results against truncated CI based on nonoptimized (red cross) or optimized (blue circles) projected 0qp, 2qp, and 4qp configurations.

is computed. Exact results are compared in Fig. 10 with those obtained from various approximate many-body methods of present interest. Again, truncated CI calculations based on (non)optimized projected 0qp and 4qp configurations provide
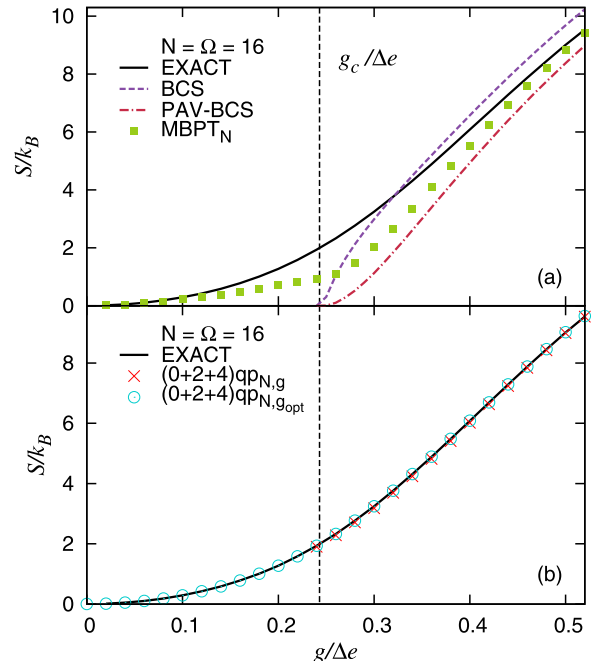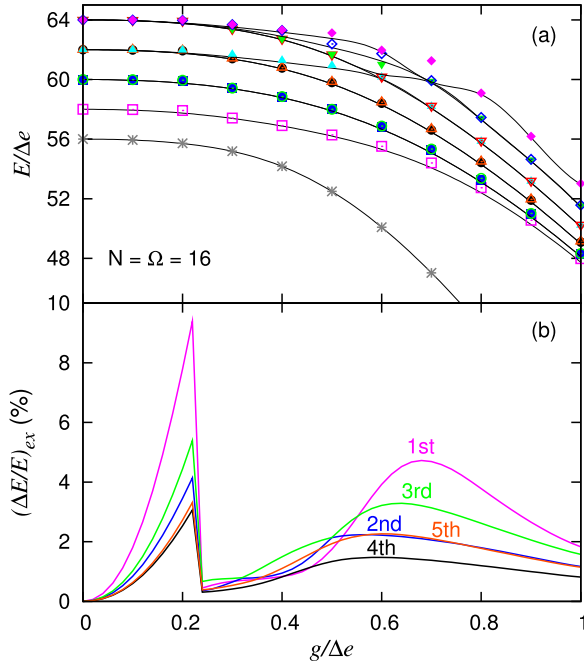

FIG. 10. Same as Fig. 9 for the one-body entropy.

FIG. 11. Low-lying excitation spectrum as a function of g obtained with $N = \Omega = 16$ and $g_{aux} = g$. Exact results are compared with truncated CI calculations based on projected 0qp, 2qp, and 4qp configurations. Upper panel shows absolute energies of the 10 lowest excited states for exact (black solid lines) and truncated CI (symbols) results. Lower panel shows relative errors on excitation energies for the five lowest excited states.

results that are below 0.1% (2%) error for all coupling strengths g ($g > g_c$) and that are much superior to the other methods shown. This demonstrates that single-particle occupation numbers across the Fermi energy are accurately described, which eventually propagate to any one-body observable.

C. Low-lying excitations

Only ground-state properties have been discussed so far. Being based on a direct diagonalization of the Hamiltonian in a restricted space, it is a tremendous advantage of the presently designed method to also access excited states. Given that the size of the subspace covered is drastically smaller than the one of $\mathcal{H}_N$, one can only expect to provide a fair account of a few low-lying states.

Energies of the 10 lowest excited seniority-zero states are compared with exact results in the upper panel of Fig. 11 for $N = \Omega = 16$ and $g_{aux} = g$. Truncated CI calculations based on projected 0qp, 2qp, and 4qp configurations provide an accurate reproduction of the low-lying spectroscopy. More specifically, the error made on the excitation energy[15] of the five lowest excited states is lower than 9.5% for $g \in [0,1]$.

---

[15]The relative error on excitation energies is given by $(\Delta E/E)_{ex} = \left(1 - \frac{E_{ex}^{approx}}{E_{ex}^{exact}}\right) \times 100\%$, where E_{ex} denotes the excitation energy of the corresponding state.
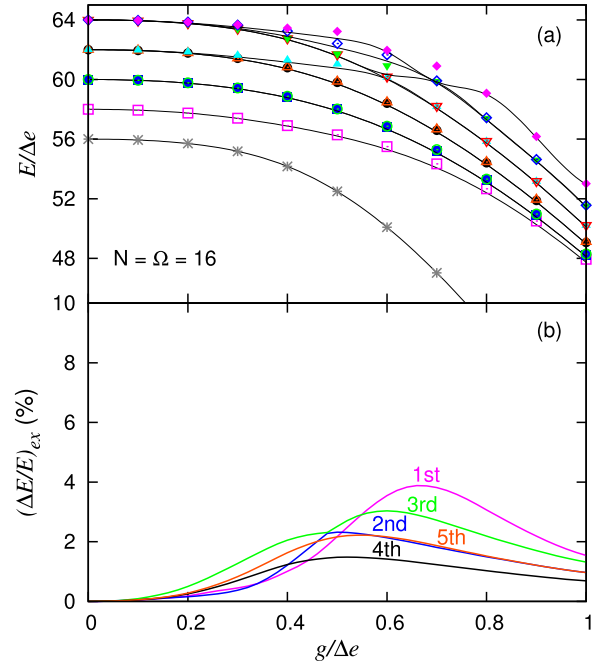

FIG. 12. Same as Fig. 11 for $g_{aux} = g_{opt}$.

The improvement of the ground-state energy obtained on the basis of Ritz' variational principle does not carry over to excited states. Still, one may explore the empirical benefit of optimizing the order parameter for low-lying excited states. The same results as in Fig. 11 are thus displayed in Fig. 12 for $g_{aux} = g_{opt}$. While no particular pattern can be anticipated for individual excited states, it happens that the reproduction of the low-lying states are overall slightly improved in the superfluid phase. But, most importantly, the relative error is divided by a factor of two in the normal phase just prior to the phase transition, i.e., in the regime of pairing fluctuations.

VII. CONCLUSIONS

A novel approximate many-body scheme is presently tested on the so-called attractive pairing Hamiltonian as a way to gauge its capacity to account for the physics of N-body systems transitioning from the weak- to the strong-coupling regime via a normal-to-superfluid phase transition. This work takes place in the context of designing polynomially scaling methods that are possibly more (i) accurate and (ii) easily applicable to more quantum states than those, i.e., Gorkov self-consistent Green's function (GSCGF), multireference in-medium similarity renormalization group (MR-IMSRG), and Bogoliubov coupled-cluster (BCC) methods, which are currently operating a breakthrough in the *ab initio* calculations of medium-mass open-shell nuclei.

The presently proposed method is variational and happens to be an interesting candidate to achieve the above-mentioned goal. It does so by combining three features that have been employed separately in various existing many-body methods so far.

(1) It is a truncated configuration-interaction method, i.e., it amounts to diagonalizing the Hamiltonian in a highly truncated subspace of the total N-body Hilbert space.

(2) The reduced Hilbert space is generated via a set of states that exploit the spontaneous [U(1)] symmetry breaking and restoration associated with the (normal-to-superfluid) quantum phase transition of the N-body system. Specifically, the set of states considered is given by the particle-number projected BCS state along with projected seniority-zero two- and four-quasiparticle excitations built on top of the BCS state. Because each basis state is symmetry projected, the method consists of representing the Schrödinger equation onto a *nonorthonormal* basis. The corresponding diagonalization can be performed by using standard techniques.

(3) The extent by which the BCS reference state breaks [U(1)] symmetry is optimized *in the presence* of projected two- and four-quasiparticle excitations. This constitutes an extension of the so-called restricted variation after projection method in use within the frame of multireference nuclear energy density functional calculations [66].

The many-body scheme has been compared with exact solutions of the attractive pairing Hamiltonian based on Richardson equations [28,31,37]. By construction, the method is exact for $N = 2$ and $N = 4$. For $N = (8, 16, 20)$, the error in the ground-state *correlation energy* is less than (0.006%, 0.1%, 0.15%) across the entire range of coupling g defining the pairing Hamiltonian and driving the normal-to-superfluid quantum phase transition. To the best of our knowledge, this is better than any many-body method scaling polynomially (N^6 here) with the system size and tested so far on the pairing Hamiltonian. In particular, it is superior to the highly accurate $PoST_\alpha$ and $PoST_x$ methods recently proposed in Ref. [59] with the same motivations as here. The presently proposed method offers the great additional advantage of automatically accessing low-lying excited states. The error in excitation energies of the five lowest excited states is less than 4% for $g \in [0,1]$ for $N = 16$.

The schematic pairing Hamiltonian employed here corresponds to modeling sub-closed-shell systems, i.e., the naive filling of the doubly degenerate picket fence single-particle scheme with an even number of particles always leads to a sub-closed-shell system. Correspondingly, the Hartree–Fock reference state can always be defined, which is mandatory to apply many methods, including the recently proposed PoST methods [59]. However, this HF reference cannot even be defined in the genuinely open-shell systems in which we are actually interested, i.e., for the vast majority of singly or doubly open-shell nuclei. The presently proposed method, however, is based on a reference state that spontaneously breaks [U(1)] symmetry whenever necessary and can be equally applied independently of the closed-shell, sub-closed-shell, or genuinely open-shell character of the system under study. This makes the method extremely versatile.

Although IMSRG and SCGF techniques have not been applied to the pairing Hamiltonian problem throughout the superfluid phase transition (while CC has), their accuracy in the best current level of implementation is of the order of a few percent error in the ground-state correlation energy of singly open-shell nuclei. In view of that, results obtained in the present work indicate that the truncated CI method based on low-order projected qp excitations constitutes an interesting method to pursue. To go beyond the present proof-of-principle calculation, our objective is to implement the method for *ab initio* calculations of mid-mass open-shell nuclei.

Last but not least, one should note that the highly accurate character of the method is achieved at the price of giving up on size extensivity. It is a common feature of all truncated CI methods that is also shared by the PoST method of Ref. [59]. The increasing relative error from 0.006% to 0.1% and to 0.15% when increasing the particle number from $N = 8$ to $N = 16$ and to $N = 20$ might already be a trace of it. Restoring size consistency demands the inclusion of very high excitation levels and possibly all excitations, which is prohibitive. Although giving up on size extensivity is somewhat unconventional from the perspective of modern many-body methods, and although it deserves attention as larger systems are studied, it is the price one is willing to pay to obtain a highly accurate description at a reasonable computational cost.

[1] S. K. Bogner, R. J. Furnstahl, S. Ramanan, and A. Schwenk, Nucl. Phys. A **773**, 203 (2006).

[2] S. Ramanan, S. K. Bogner, and R. J. Furnstahl, Nucl. Phys. A **797**, 81 (2007).

[3] S. K. Bogner, R. J. Furnstahl, and A. Schwenk, Prog. Part. Nucl. Phys. **65**, 94 (2010).

[4] I. Shavitt and R. J. Bartlett, *Many-Body Methods in Chemistry and Physics* (Cambridge University Press, Cambridge, 2009).

[5] G. Hagen, T. Papenbrock, M. Hjorth-Jensen, and D. J. Dean, Rep. Prog. Phys. **77**, 096302 (2014).

[6] W. H. Dickhoff and C. Barbieri, Prog. Part. Nucl. Phys. **52**, 377 (2004).

[7] A. Cipollone, C. Barbieri, and P. Navrátil, Phys. Rev. Lett. **111**, 062501 (2013).

[8] H. Hergert, S. K. Bogner, T. D. Morris, A. Schwenk, and K. Tsukiyama, Phys. Rep. **621**, 165 (2016).

[9] G. R. Jansen, J. Engel, G. Hagen, P. Navratil, and A. Signoracci, Phys. Rev. Lett. **113**, 142502 (2014).

[10] S. K. Bogner, H. Hergert, J. D. Holt, A. Schwenk, S. Binder, A. Calci, J. Langhammer, and R. Roth, Phys. Rev. Lett. **113**, 142501 (2014).

[11] M. Bender, P.-H. Heenen, and P.-G. Reinhard, Rev. Mod. Phys. **75**, 121 (2003).

[12] C. Yannouleas and U. Landman, Rep. Prog. Phys. **70**, 2067 (2007).

[13] T. Duguet, Lect. Notes Phys. **879**, 293 (2014).

[14] V. Somà, T. Duguet, and C. Barbieri, Phys. Rev. C **84**, 064317 (2011).

[15] V. Somà, C. Barbieri, A. Cipollone, T. Duguet, and P. Navrátil, EPJ Web Conf. **66**, 02005 (2014).

[16] V. Lapoux, V. Somá, C. Barbieri, H. Hergert, J. D. Holt, and S. R. Stroberg, Phys. Rev. Lett. **117**, 052501 (2016).

[17] H. Hergert, S. Binder, A. Calci, J. Langhammer, and R. Roth, Phys. Rev. Lett. **110**, 242501 (2013).

[18] H. Hergert, Phys. Scr. **92**, 023002 (2017).

[19] A. Signoracci, T. Duguet, G. Hagen, and G. R. Jansen, Phys. Rev. C **91**, 064320 (2015).

[20] F. Barranco, R. Broglia, G. Colo', E. Vigezzi, and P. Bortignon, Eur. Phys. J. A **21**, 57 (2004).

[21] A. Idini, F. Barranco, E. Vigezzi, and R. Broglia, J. Phys.: Conf. Ser. **312**, 092032 (2011).

[22] T. Lesinski, T. Duguet, K. Bennaceur, and J. Meyer, Eur. Phys. J. A **40**, 121 (2009).

[23] T. Duguet, *Fifty Years of Nuclear BCS Theory*, edited by R. Broglia and V. Zelevinsky (World Scientific, Singapore, 2013), p. 229.

[24] D. Lacroix and D. Gambacurta, Phys. Rev. C **86**, 014306 (2012).

[25] T. Duguet and A. Signoracci, J. Phys. G **44**, 015103 (2016).

[26] V. Somà, A. Cipollone, C. Barbieri, P. Navrátil, and T. Duguet, Phys. Rev. C **89**, 061301(R) (2014).

[27] H. Hergert, S. K. Bogner, T. D. Morris, S. Binder, A. Calci, J. Langhammer, and R. Roth, Phys. Rev. C **90**, 041302 (2014).

[28] R. W. Richardson and N. Sherman, Nucl. Phys. **52**, 221 (1964).

[29] R. W. Richardson, Phys. Rev. **141**, 949 (1966).

[30] R. W. Richardson, J. Math. Phys. **9**, 1327 (1968).

[31] J. Dukelsky, S. Pittel, and G. Sierra, Rev. Mod. Phys. **76**, 643 (2004).

[32] A. Volya, B. A. Brown, and V. Zelevinsky, Phys. Lett. B **509**, 37 (2001).

[33] V. Zelevinsky and A. Volya, Phys. At. Nucl. **66**, 1781 (2003).

[34] T. Sumaryada and A. Volya, Phys. Rev. C **76**, 024319 (2007).

[35] R. Capote, E. Mainegra, and A. Ventura, J. Phys. G **24**, 1113 (1998).

[36] A. Mukherjee, Y. Alhassid, and G. F. Bertsch, Phys. Rev. C **83**, 014319 (2011).

[37] K. Van Houcke, S. M. A. Rombouts, and L. Pollet, Phys. Rev. E **73**, 056703 (2006).

[38] P. W. Claeys, S. De Baerdemacker, M. Van Raemdonck, and D. Van Neck, Phys. Rev. B **91**, 155102 (2015).

[39] J. Dukelsky, G. G. Dussel, J. G. Hirsch, and P. Schuck, Nucl. Phys. A **714**, 63 (2003).

[40] K. Dietrich, H. J. Mang, and J. H. Pradal, Phys. Rev. **135**, B22 (1964).

[41] P. G. de Gennes, *Superconductivity of Metals and Alloys* (Benjamin, New York, 1966).

[42] J. L. Egido and P. Ring, Nucl. Phys. A **383**, 189 (1982).

[43] J. L. Egido and P. Ring, Nucl. Phys. A **388**, 19 (1982).

[44] J. Blaizot and G. Ripka, *Quantum Theory of Finite Systems* (MIT Press, Cambridge, 1986).

[45] P.-H. Heenen, P. Bonche, J. Dobaczewski, and H. Flocard, Nucl. Phys. A **561**, 367 (1993).

[46] J. A. Sheikh and P. Ring, Nucl. Phys. A **665**, 71 (2000).

[47] M. Anguiano, J. L. Egido, and L. M. Robledo, Nucl. Phys. A **696**, 467 (2001).

[48] N. Sandulescu and G. F. Bertsch, Phys. Rev. C **78**, 064318 (2008).

[49] G. Hupin and D. Lacroix, Phys. Rev. C **83**, 024317 (2011).

[50] H. Molique and J. Dudek, Phys. Rev. C **56**, 1795 (1997).

[51] H. Molique and J. Dudek, *Zakopane Conference on Nuclear Physics, Sep 2006, Poland* (Jagiellonian University, Cracow, 2007), Vol. 38, pp. 1405–1409.

[52] N. Pillet, N. Sandulescu, N. V. Giai, and J.-F. Berger, Phys. Rev. C **71**, 044306 (2005).

[53] P. A. Johnson, P. Ayers, P. A. Limacher, S. D. Baerdemacker, D. V. Neck, and P. Bultinck, Comput. Theor. Chem. **1003**, 101 (2013).

[54] P. A. Limacher, P. Ayers, P. A. Johnson, S. D. Baerdemacker, D. V. Neck, and P. Bultinck, J. Chem. Theory Comput. **9**, 1394 (2013).

[55] T. Stein, T. M. Henderson, and G. E. Scuseria, J. Chem. Phys. **140**, 214113 (2014).

[56] T. M. Henderson, I. W. Bulik, T. Stein, and G. E. Scuseria, J. Chem. Phys. **141**, 244104 (2014).

[57] T. M. Henderson, G. E. Scuseria, J. Dukelsky, A. Signoracci, and T. Duguet, Phys. Rev. C **89**, 054305 (2014).

[58] J. Dukelsky, S. Pittel, and C. Esebbag, Phys. Rev. C **93**, 034313 (2016).

[59] M. Degroote, T. M. Henderson, J. Zhao, J. Dukelsky, and G. E. Scuseria, Phys. Rev. B **93**, 125124 (2016).

[60] P. Ring and P. Schuck, *The Nuclear Many-Body Problem* (Springer-Verlag, New York, 1980).

[61] D. M. Brink and R. A. Broglia, *Nuclear Superfluidity: Pairing in Finite Systems* (Cambridge University Press, Cambridge, 2005).

[62] D. Gambacurta and D. Lacroix, Phys. Rev. C **86**, 064320 (2012).

[63] K. Allaart, E. Boeker, G. Bonsignori, M. Savoia, and Y. Gambhir, Phys. Rep. **169**, 209 (1988).

[64] M. A. Caprio, F. Q. Luo, K. Cai, C. Constantinou, and V. Hellemans, J. Phys. G **39**, 105108 (2012).

[65] C. Møller and M. S. Plesset, Phys. Rev. **46**, 618 (1934).

[66] T. R. Rodríguez, J. L. Egido, and L. M. Robledo, Phys. Rev. C **72**, 064303 (2005).

[67] A. Himeda and M. Ogata, Phys. Rev. Lett. **85**, 4345 (2000).

[68] M. Capello, F. Becca, M. Fabrizio, S. Sorella, and E. Tosatti, Phys. Rev. Lett. **94**, 026406 (2005).

[69] G. Hupin, D. Lacroix, and M. Bender, Phys. Rev. C **84**, 014309 (2011).

[70] J. von Delft, A. D. Zaikin, D. S. Golubev, and W. Tichy, Phys. Rev. Lett. **77**, 3189 (1996).

[71] F. Braun and J. von Delft, Phys. Rev. Lett. **81**, 4712 (1998).